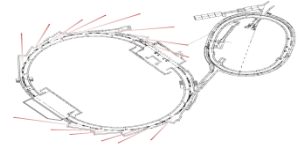# Beam Size Measurement

○ **Survey of beam size measurement techniques and applications.**

○ **Detailed analysis of an X-Ray pinhole camera**

   ↳ **Description**

   ↳ **What is actually measured?**

   ↳ **Image processing and resolution**
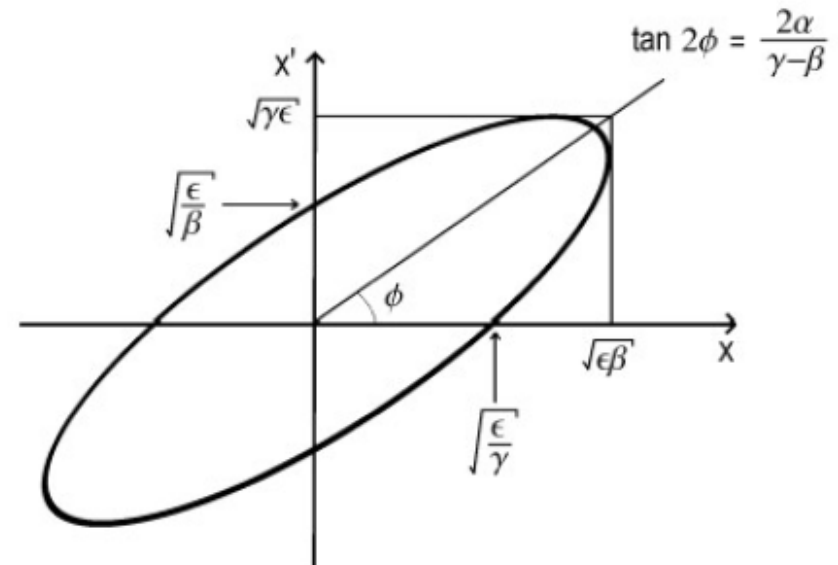
Gaussian beam profile

- **Electrons in storage ring damp to 2D Gaussian distribution.**

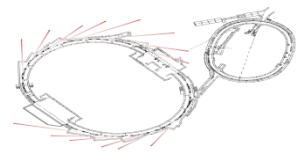$$A_0 \exp\left(-\frac{\beta x'^2 + 2\alpha x x' + \gamma x^2}{2\varepsilon}\right)$$

$$\sigma_x = \sqrt{\beta_x \varepsilon_x}$$
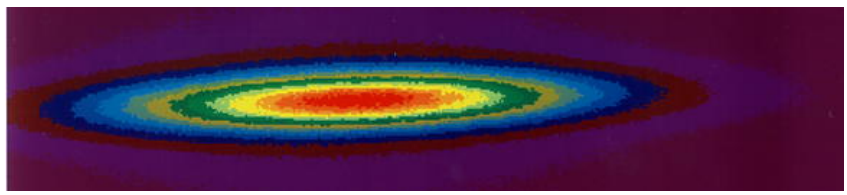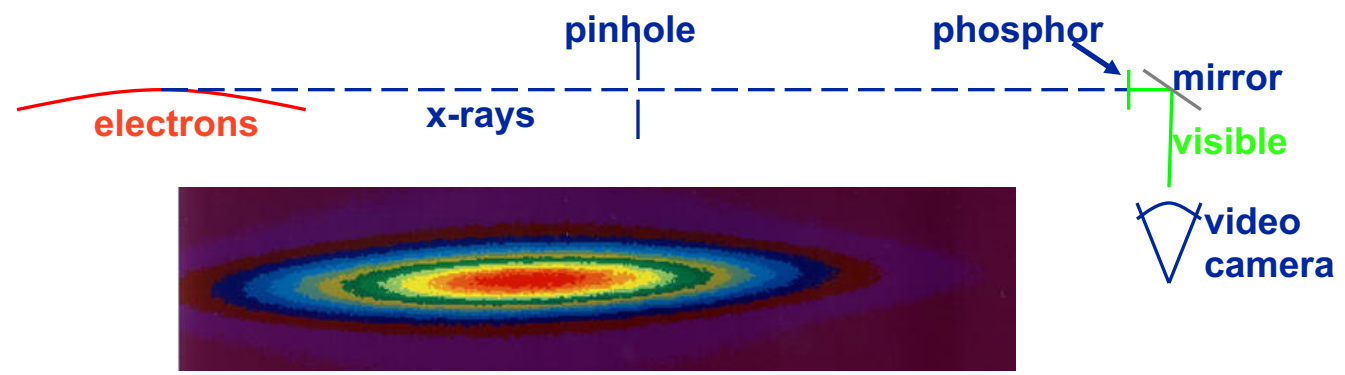
$$\sigma_x' = \sqrt{\gamma_x \varepsilon_x}$$

- **Similar distribution in y.**

$$\tan 2\phi = \frac{2\alpha}{\gamma - \beta}$$

Beam size measurements

X-Ray pinhole camera

pinhole   **phosphor**   **mirror**

electrons   **x-rays**   **visible**

video camera

Pinhole camera array

(Kuske et al., Bessy)

Phosphor screen

Al filter   Pinhole array $\cdot \cdot \phi d$ Source

Intensity R_2 R_1

Pixel number — 400, 300, 200, 100, 0

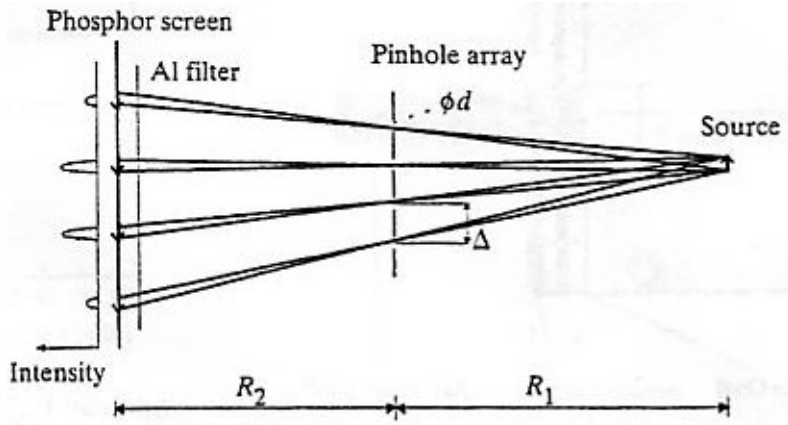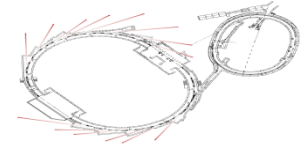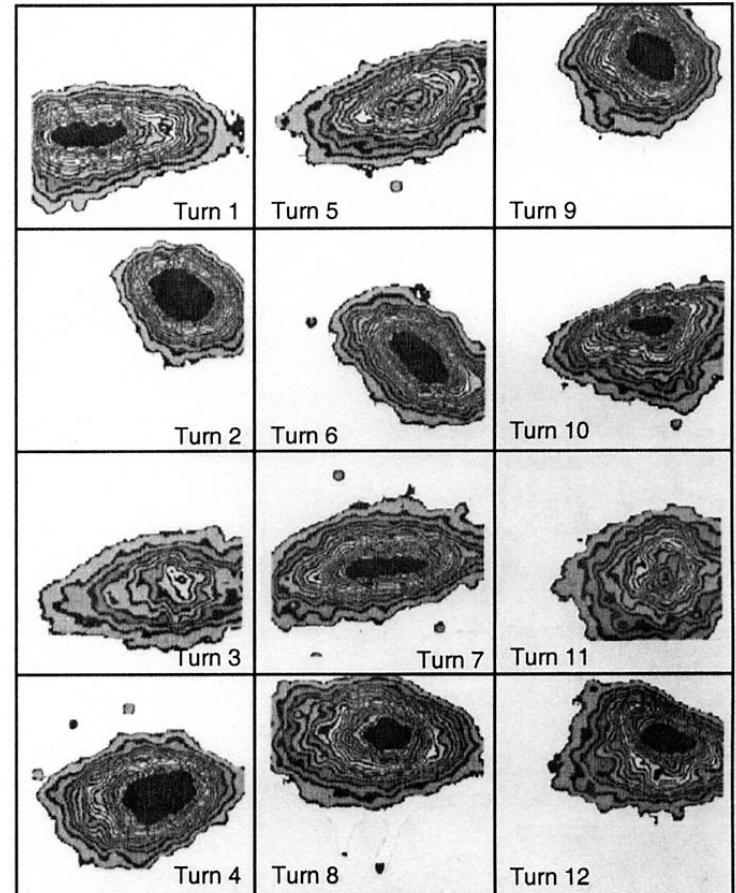0 10 20 30 40 50 60 70 80
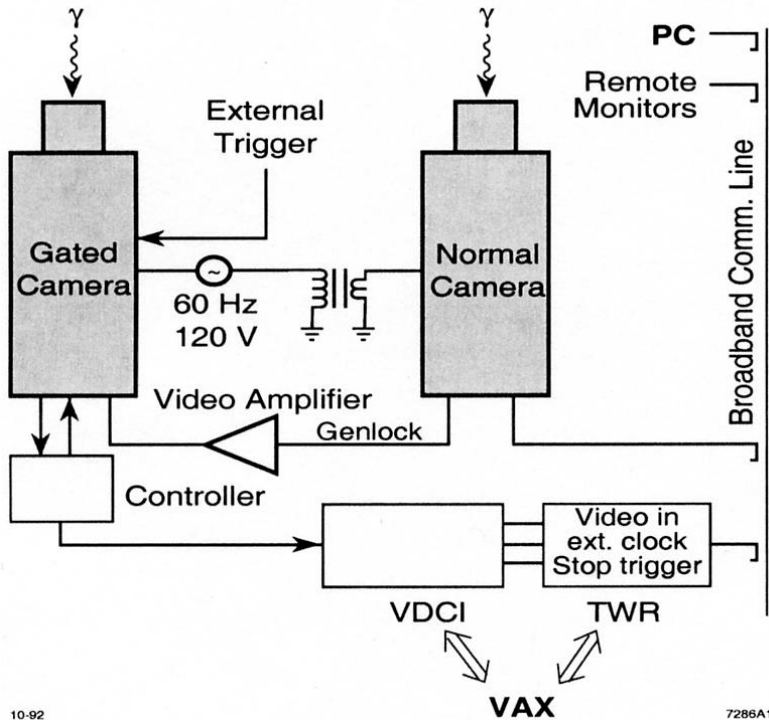Intensity (grey levels)
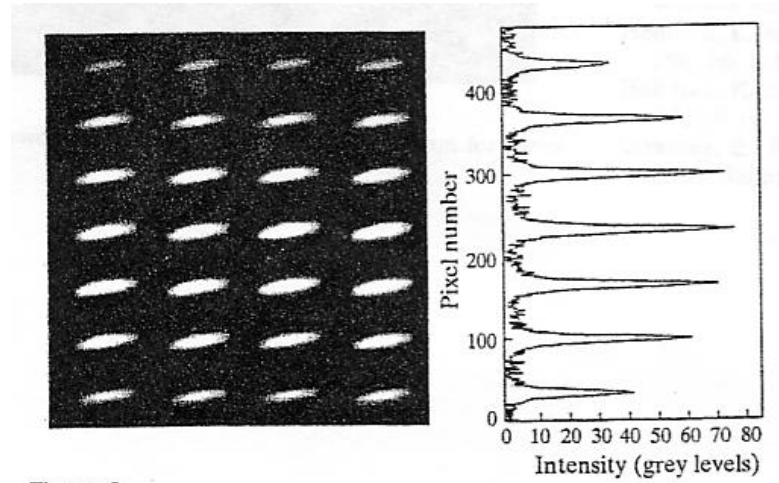
Figure 2
Left: image of a portion of the phosphor observed on a BESSY I bending magnet. Right: integrated intensities of one column of images on the phosphor.

Turn-by-turn monitor

Turn-by-turn measurements of synchrotron radiation are used for measuring beam instability and injection mis-match.
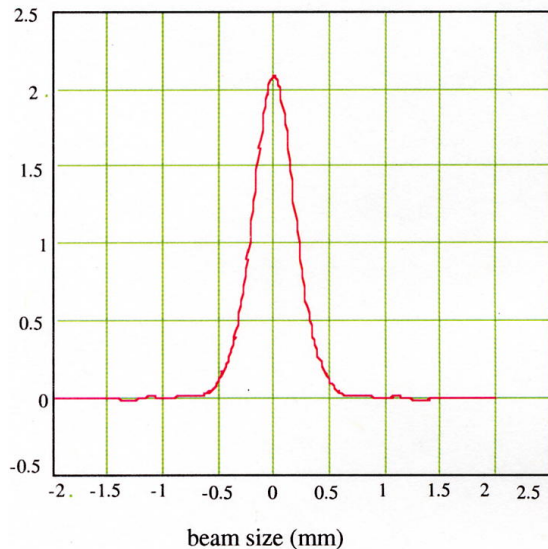
Minty and Spence, PAC'95

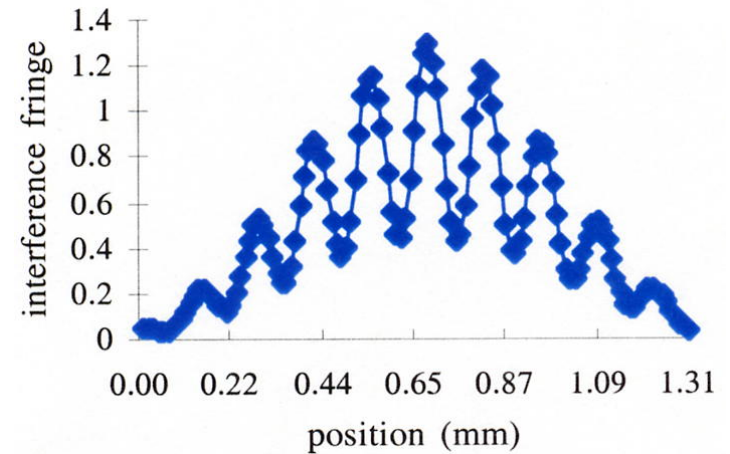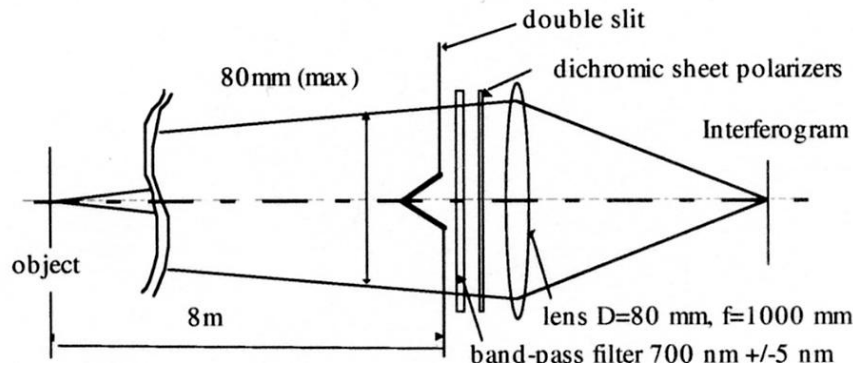# Beam size measurement, spatial coherence
(Mitsuhashi, PAC97)

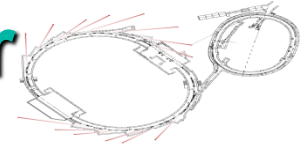**Michelson's method for measuring the size of stars applied to measuring electron beam size. Spatial cohence increases as beam size decreases.**
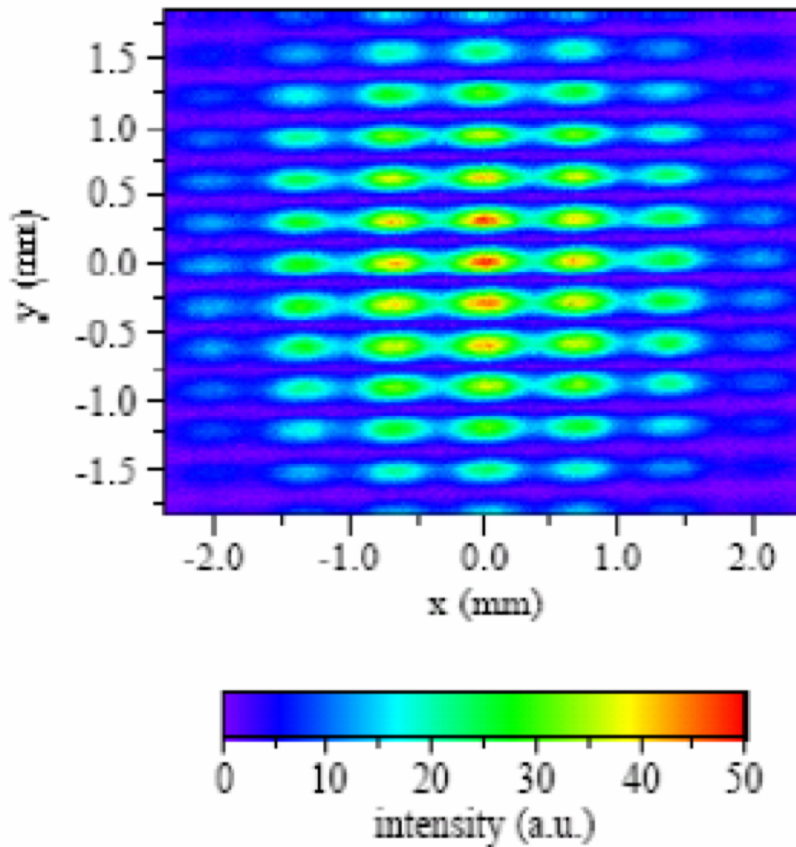

Vertical beam size can be obtained from the Fourier transform of the degree of spatial coherence.

2D visible light interferometer

M.Masaki and S.Takano,
J.Synchrotron Rad. 10 (2003) 295

π-mode SR beam size measurement

○ **Image vertically polarized SR**

○ **Intensity at y=0 determined by ε_y**

○ **Andersson et al., NIMA 591 (2008).**

○ **Angela Saa Hernandez, ALERT 2014 Workshop**

$\sigma_{ey} = 9.0\ \mu m$

$\sigma_{ey} = 6.4\ \mu m$

$\sigma_{ey} = 0$

measured

Vertical position

air

vacuum

blades to set horizontal acceptance

fused silica window

grey filter / polarizer / band pass

aluminized flat mirror

CCD

BX-09

pinhole array

electron beam

fused silica lens

X-ray branch

visible branch

finger absorber

SiC flat mirror

aluminium window molybdenum filter phosphor screen

zoom lens

CCD
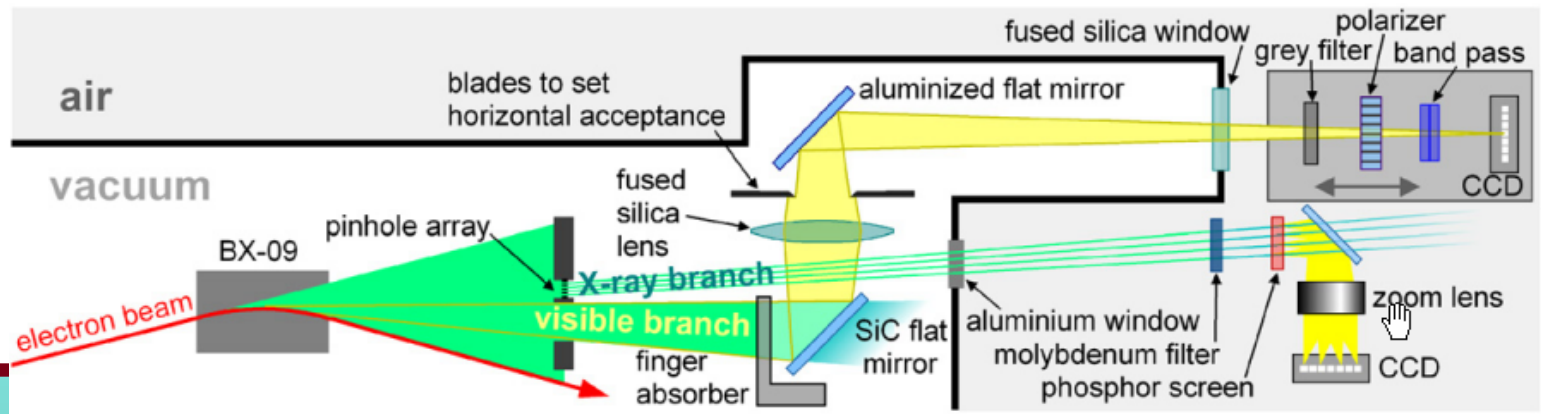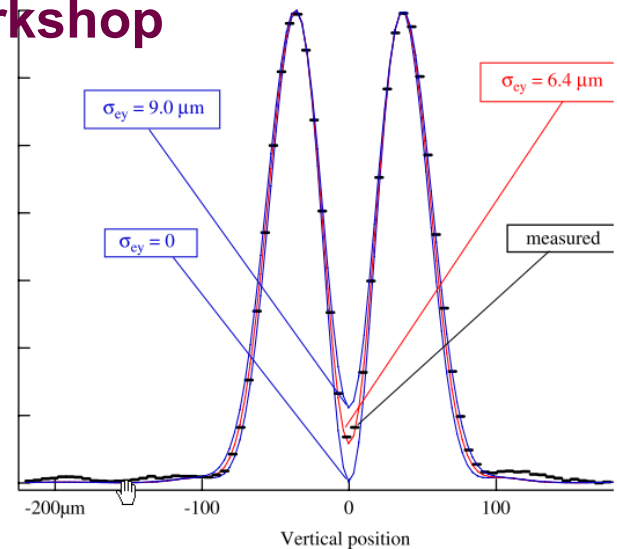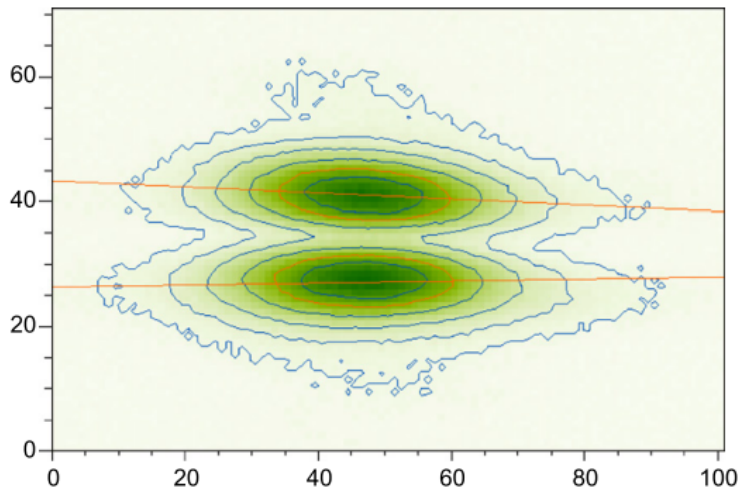
Vertical emittance measurement in Australia with vertical undulator

(a) (b) (c) (d)
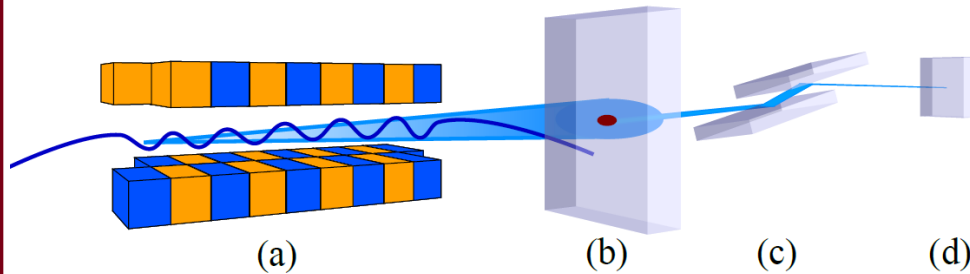
6th harmonic, pm rad emittance
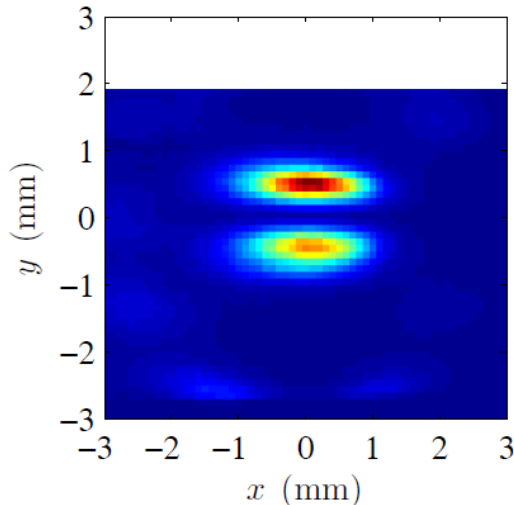
Measured   **Simulation**
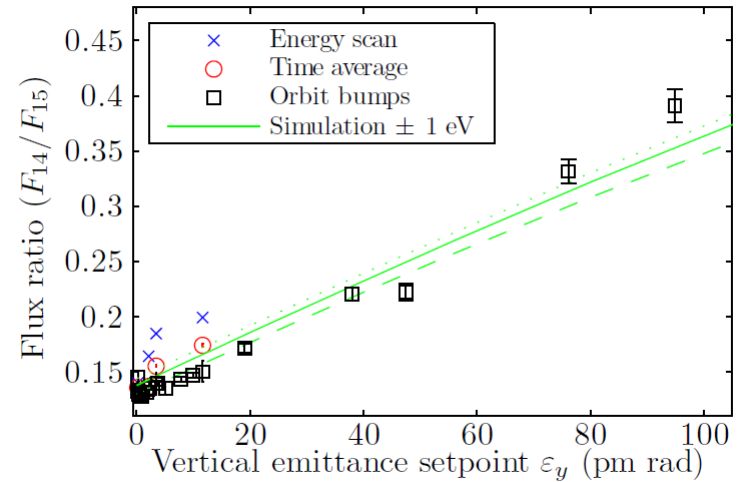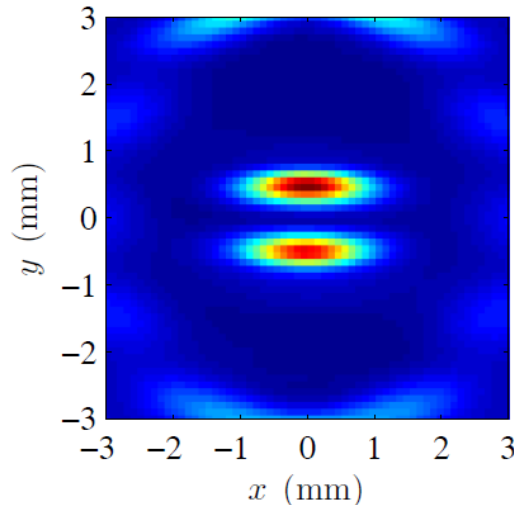
- **Useful pm rad emittance monitor**
- **Non-Gaussian radiation distribution**

Kent Wootton, thesis (2014): http://hdl.handle.net/11343/39616

Beam size measurements
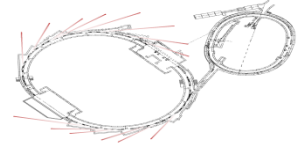
Touschek lifetime

$$\tau_{T_{1/2}} \propto \text{bunch volume}$$

Lifetime with 80 mA in a single bunch.
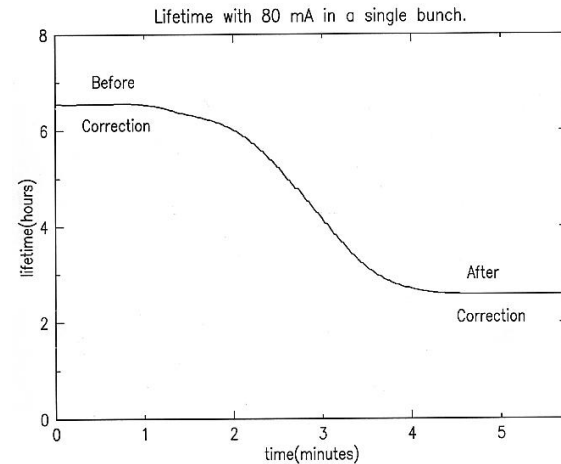
Scrapers measure beam halo

Peter Stefan et al., NIMA, 1998

halo, Coulomb scattering

□ experiment
— theory

core, $\sigma_y = 20\mu m$

(a)

□ experiment
— theory

core, $\sigma_y = 7\mu m$

(b)
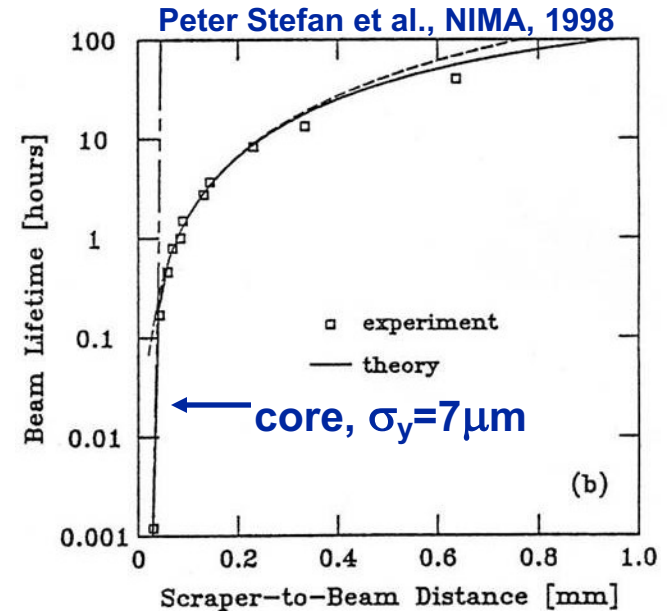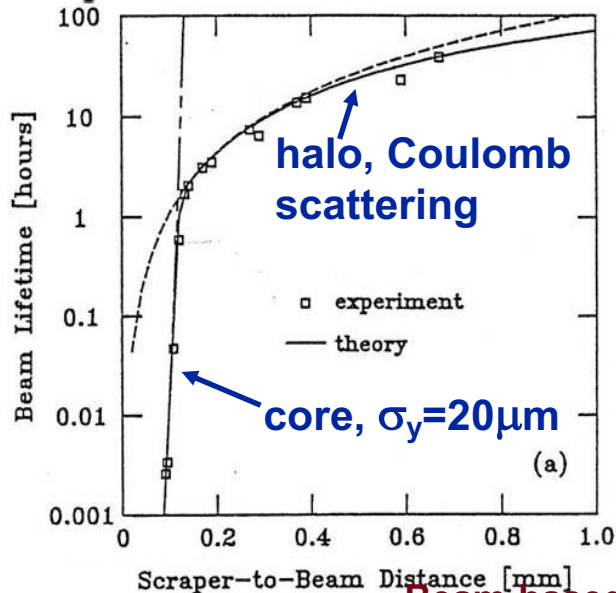
Laser wire beam size measurement
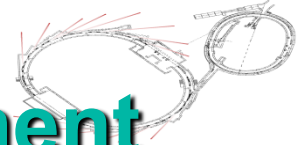
A laser wire successfully measured very small beam sizes at KEK ATF, H. Sakai et al., PRST-AB Volume 5 (2002)

(Expanded view of laser wire region)

Photon detector system

Laser wire system

Scattered

Bending Magnet

electron

Optical cavity

electron

Laser

CsI(pure) Scintillator

φ5mm Pb collimator

Movable table

Laser wire region

ATF damping ring

1.28 GeV linac
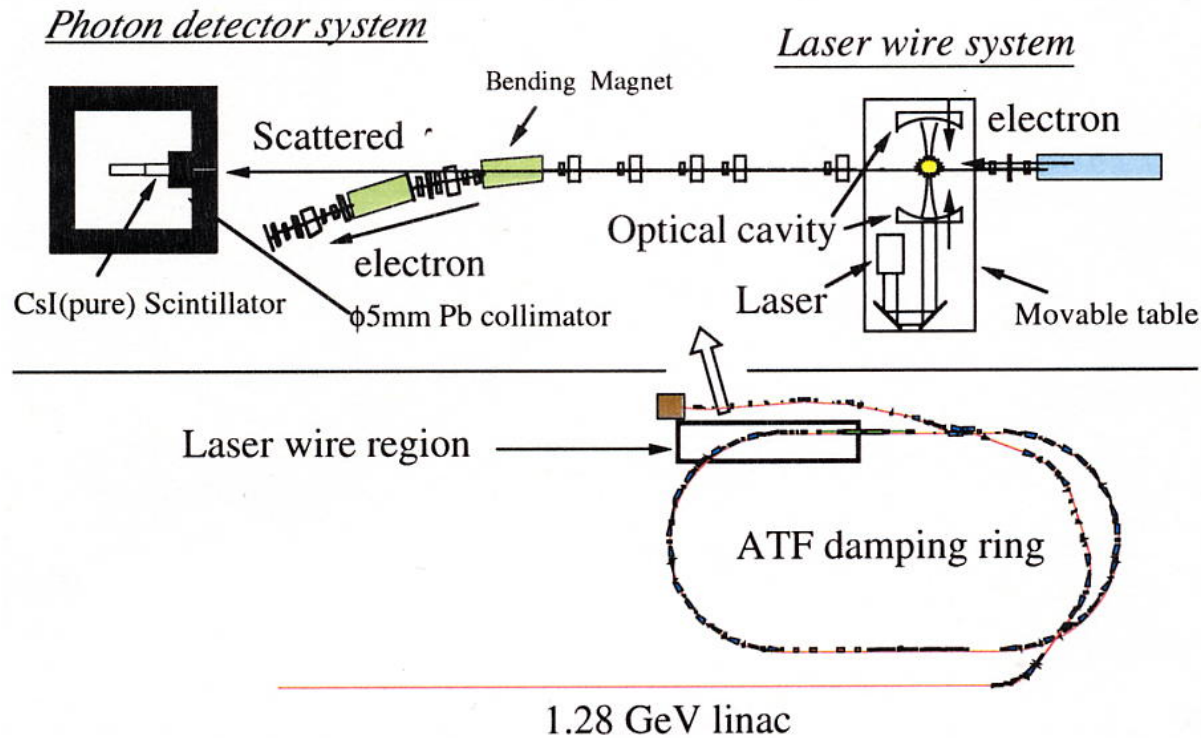
Measures of beam size

oLuminosity scan (Y. Cai, EPAC'00, p 400)

$\sigma_x = 194 +- 3 \ \mu m$
$\sigma_y = 3.7 +- 0.2 \ \mu m$

Correction Optimum :
14.9 +- 0.2 μm
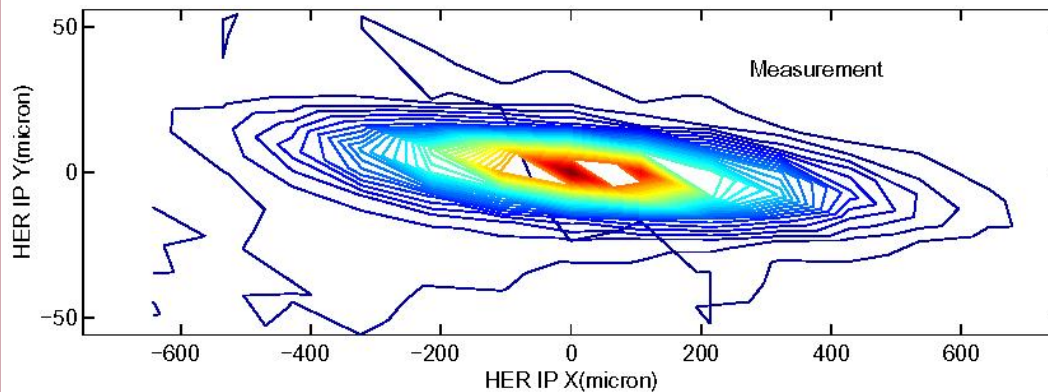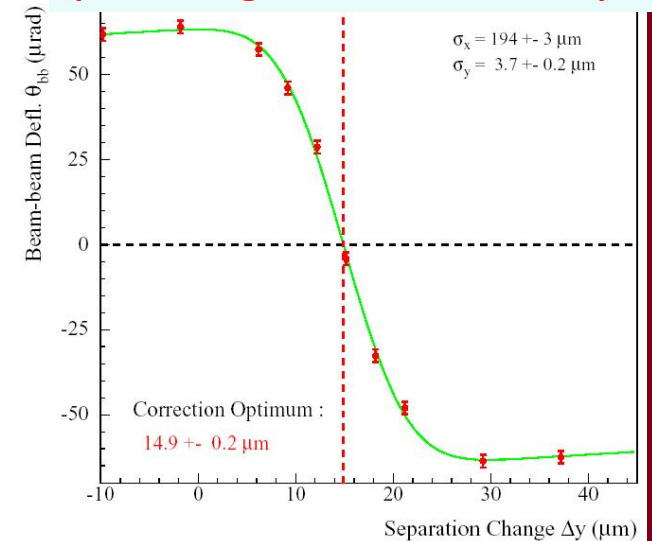
oQuadrupole moment detectors

stripline

RF cavities

(A. Jansson et al., CERN-PS, PAC'99)

Q. Luo et al., MOP176, PAC11.

N. Barov, Far-Tech

Beam size measurement   Beam-based Diagnostics, USPAS, January 21-25, 2019, J. Safranek
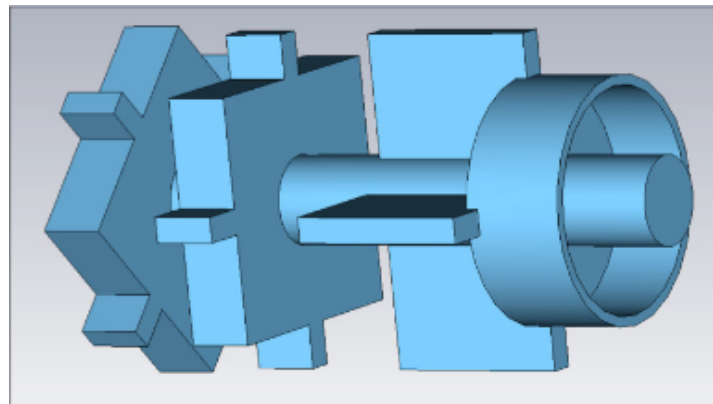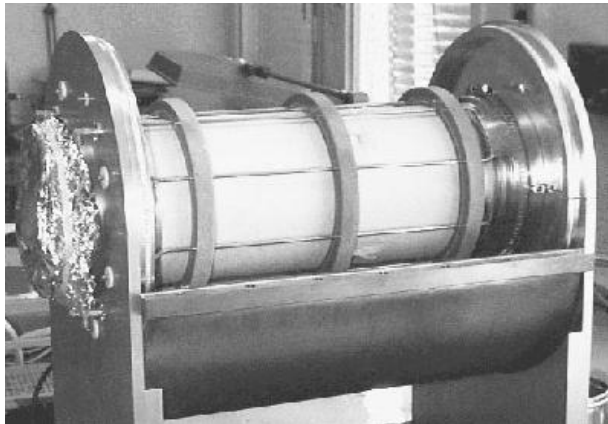
Measurement of the Transverse Beam Emittance

Method I: quadrupole scan

Principle: with a well-centered
beam, measure the beam size
as a function of the quadrupole
field strength

Here
Q is the transfer matrix of the quadrupole
R is the transfer matrix between the quadrupole
and the beam size detector
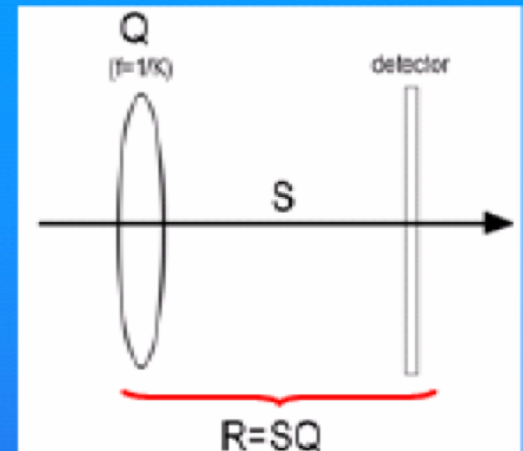
With $Q = \begin{pmatrix} 1 & 0 \\ K & 1 \end{pmatrix}$ then $R = \begin{pmatrix} S_{11} + KS_{12} & S_{12} \\ S_{21} + KS_{22} & S_{22} \end{pmatrix}$ with $\Sigma_{\text{beam}} = R\Sigma_{\text{beam},0} R^t$

The (11)-element of the beam transfer matrix is found after algebra
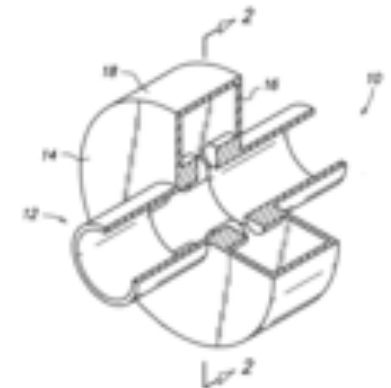to be:

$$\Sigma_{11}(= \langle x^2 \rangle) = (S_{11}{}^2 \Sigma_{11_0} + 2S_{11}S_{12}\Sigma_{12_0} + S_{12}{}^2 \Sigma_{22_0})$$
$$+ (2S_{11}S_{12}\Sigma_{11_0} + 2S_{12}{}^2 \Sigma_{12_0})K + S_{12}{}^2 \Sigma_{11_0}K^2$$

which is quadratic in the field strength, K

M. Minty, F. Zimmermann

Measurement: measure beam size versus quadrupole field strength

recall:

$$\Sigma_{11}(=\langle x^2 \rangle) = (S_{11}^2 \Sigma_{11_o} + 2S_{11}S_{12}\Sigma_{12_o} + S_{12}^2 \Sigma_{22_o})$$
$$+ (2S_{11}S_{12}\Sigma_{11_o} + 2S_{12}^2 \Sigma_{12_o})K + S_{12}^2 \Sigma_{11_o}K^2$$

data:
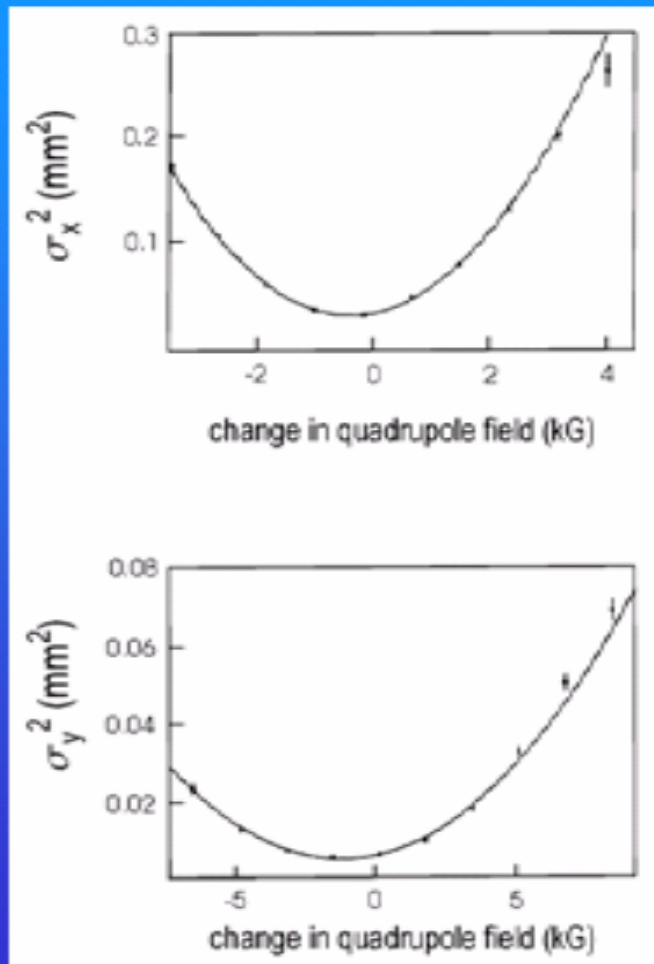
fitting function (parabolic):

$$\Sigma_{11} = A(K-B)^2 + C$$
$$= AK^2 - 2ABK + (C + AB^2)$$

equating terms (drop subscripts 'o'),

$$A = S_{12}^2 \Sigma_{11},$$

$$-2AB = 2S_{11}S_{12}\Sigma_{11} + 2S_{12}^2 \Sigma_{12},$$

$$C + AB^2 = S_{11}^2 \Sigma_{11} + 2S_{11}S_{12}\Sigma_{12} + S_{12}^2 \Sigma_{22}$$

solving for the beam matrix elements:

$$\Sigma_{11} = A/S_{12}^2,$$

$$\Sigma_{12} = -\frac{A}{S_{12}^2}\left(B + \frac{S_{11}}{S_{12}}\right),$$

$$\Sigma_{22} = \frac{1}{S_{12}^2}\left[(AB^2 + C) + 2AB\left(\frac{S_{11}}{S_{12}}\right) + A\left(\frac{S_{11}}{S_{12}}\right)^2\right]$$

M. Minty, F. Zimmermann

Determining ε_y from measured $\langle y^2 \rangle$
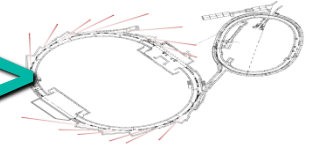
○ **ESRF – many beam size diagnostics**

○ **See differing σ^2_y/β_y at each location**

○ **For details, see Christoph's coupling lecture**

○ **A. Franchi et al., PRST-AB-14-012804 (2011).**

Measurable apparent emittance: $\mathbb{E}_y(s) = \dfrac{\sigma_y^2(s)}{\beta_y(s)} = \dfrac{\langle y^2(s) \rangle - (\delta D_y(s))^2}{\beta_y(s)}$

Non measurable projected emittance: $\epsilon_y(s) = \sqrt{\sigma_y(s)\sigma_p(s) - \sigma_{yp}^2(s)}$
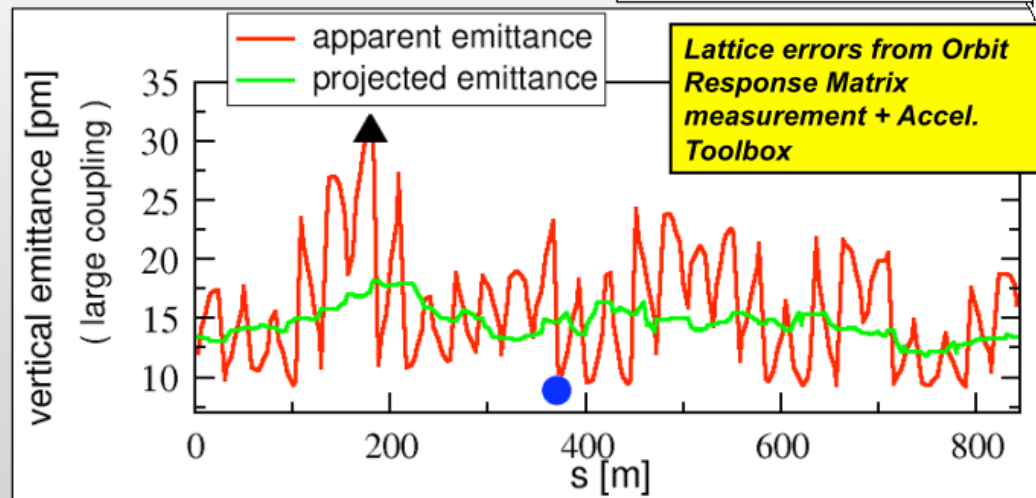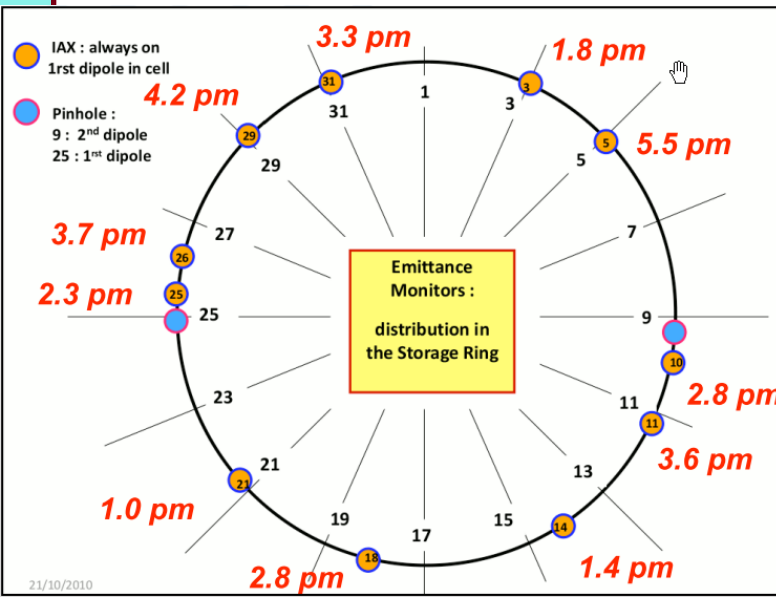
X-Ray pinhole camera

Pinhole camera on X28 dipole beamline at NSLS X-Ray Ring:

←——— 7.5 m ———→ ←——— 9.3 m ———→

electrons

x-rays   **x-rays**

mirror

visible

pinhole: molybdenum crossed slits

X-rays exit vacuum chamber through 250 μm Be window.

video camera

25 μm Al foil to harden spectrum.

YAG phosphor

Slit gap set to 30 μm and confirmed by measuring diffraction from HeNe laser.

Slit has angles to avoid internal x-ray reflections.

H_2O-cooled Cu pre-absorber takes heat load.

What is measured?

o | L2
L1 | i
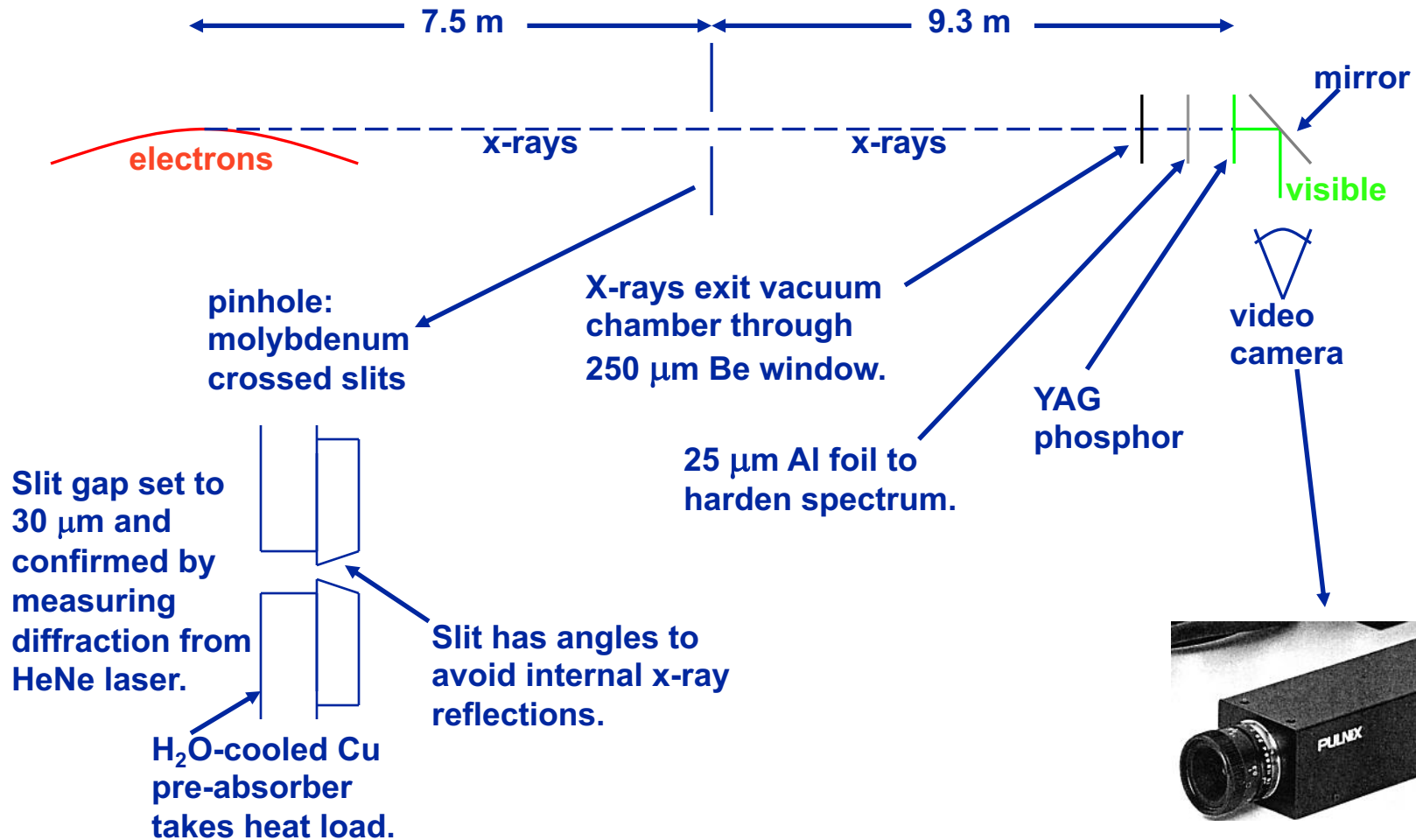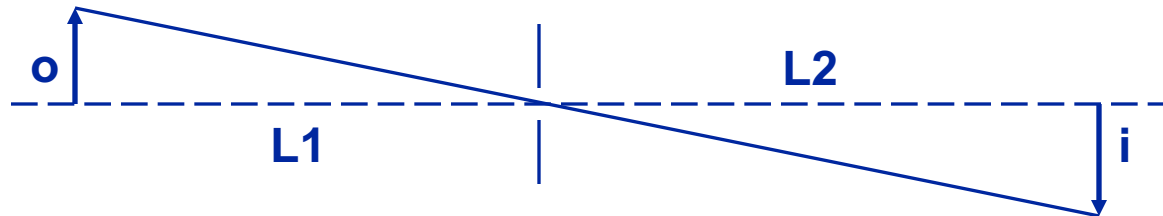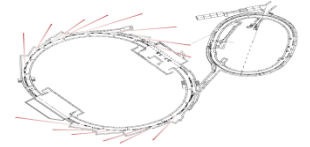
The standard formula for a pinhole camera, $i=(L2/L1)o$, assumes that the object is radiating light equally in all directions. Synchrotron radiation is highly collimated in the direction of the electrons, so this formula does not necessarily hold.

I'll show that for a dipole beamline, it does hold in the horizontal plane, but does not in general in the vertical plane.

The problem in the vertical plane is that electrons at the top of "o" (in this case the top of the electron beam) do not necessarily radiate photons that go through the pinhole, so $i<(L2/L1)o$.

Review of electron phase space
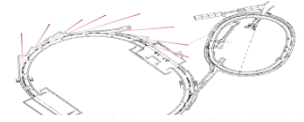
The on-energy electrons in a storage ring make a Gaussian in phase space. Area of $e^{-1/2}$ ellipse is ϵ.

$$\exp\left(-\frac{\gamma x^2 + 2\alpha xx' + \beta x'^2}{2\epsilon}\right)$$

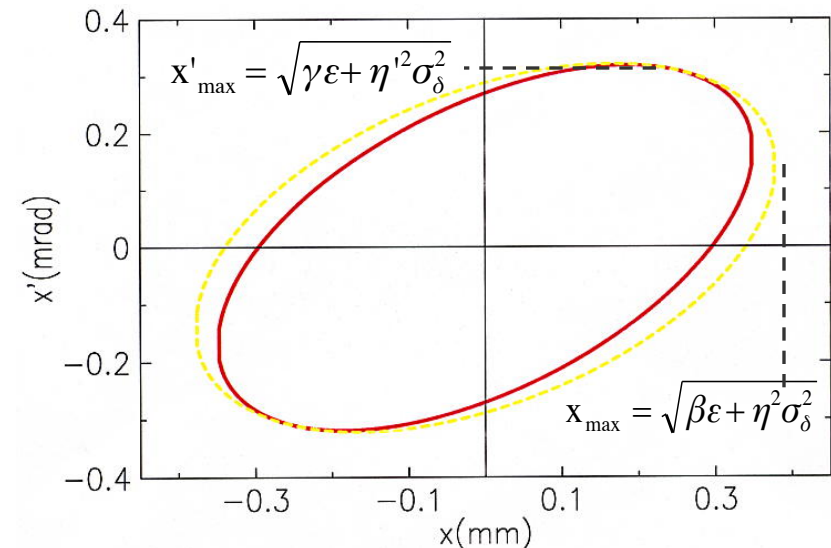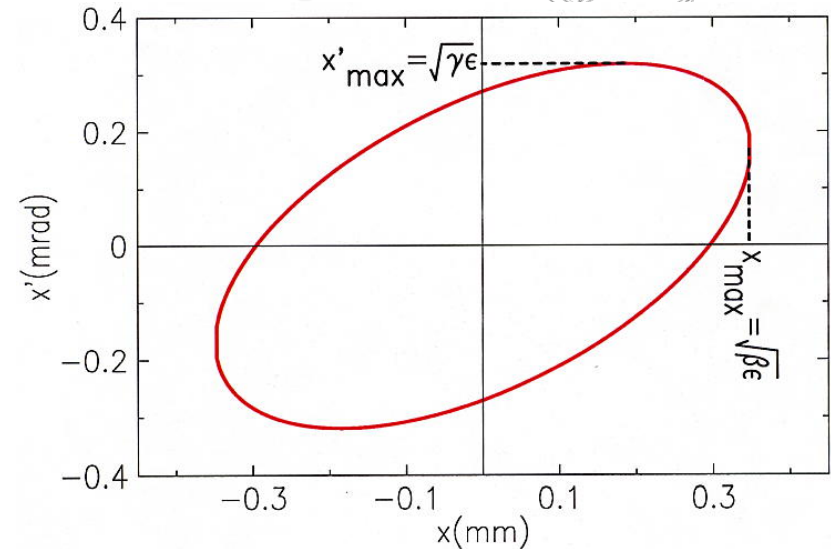$$\alpha = -\frac{\beta'(s)}{2}, \qquad \gamma = \frac{1+\alpha^2}{\beta}$$

The full extent of the electron beam including energy spread is larger.

$$\bar{\epsilon} = \epsilon\bar{\kappa}, \qquad \bar{\alpha} = \frac{\alpha - \frac{\eta\eta'\sigma_\delta^2}{\epsilon}}{\bar{\kappa}}$$

$$\bar{\beta} = \frac{\beta + \frac{\eta^2\sigma_\delta^2}{\epsilon}}{\bar{\kappa}}, \qquad \bar{\gamma} = \frac{\gamma + \frac{\eta'^2\sigma_\delta^2}{\epsilon}}{\bar{\kappa}}$$

$$\bar{\kappa} \equiv \sqrt{1 + \frac{\sigma_\delta^2}{\epsilon}(\gamma\eta^2 + 2\alpha\eta\eta' + \beta\eta'^2)}.$$

$$x'_{max} = \sqrt{\gamma\epsilon}$$
$$x_{max} = \sqrt{\beta\epsilon}$$

$$x'_{max} = \sqrt{\gamma\epsilon + \eta'^2\sigma_\delta^2}$$
$$x_{max} = \sqrt{\beta\epsilon + \eta^2\sigma_\delta^2}$$

photon ellipse at source point

Full e- ellipse with energy spread

on-energy e-

Start with on-energy electron ellipse

$$\exp\left(-\frac{\gamma x^2 + 2\alpha xx' + \beta x'^2}{2\epsilon}\right)$$

Add energy spread, σ_δ

$\otimes$

$$\exp\left(-\frac{x^2}{2\eta^2\sigma_\delta^2}\right)\delta(\eta' x - \eta x')$$

Add photon opening angle, $\sigma_{r'} = \frac{.565}{\gamma_0}\left(\frac{E_c}{E}\right)^{.425}$

$\otimes$

$$\exp\left(-\frac{x'^2}{2\sigma_{r'}^2}\right)\delta(x)$$

$$\sigma_r = \frac{\lambda}{4\pi\sigma'_r} \approx 0$$

Photon ellipse at source
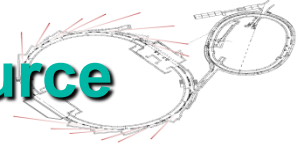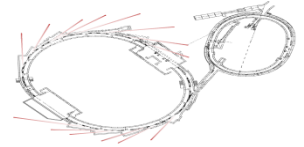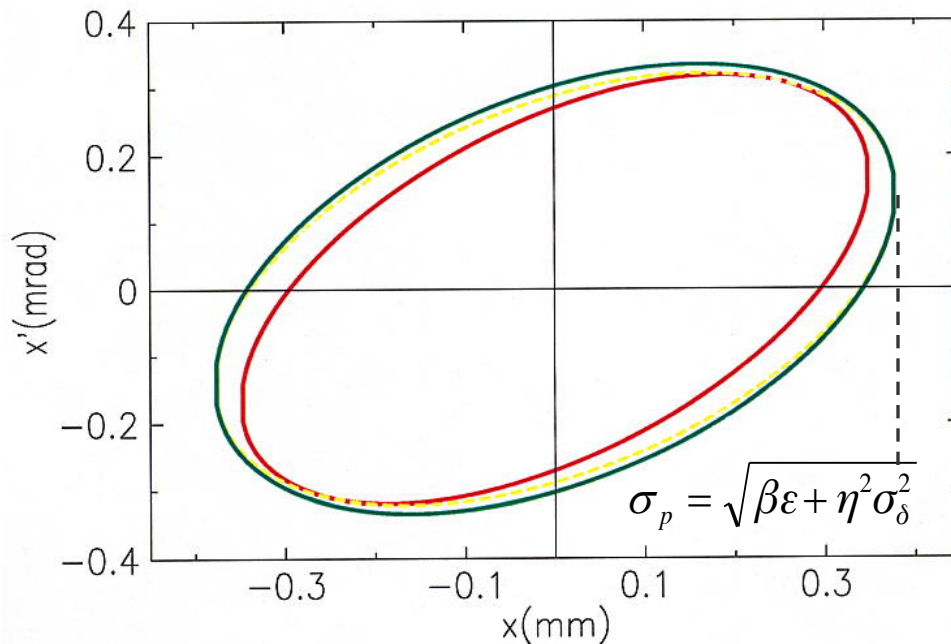
$$\epsilon_p = \epsilon\kappa, \qquad \alpha_p = \frac{\alpha - \frac{\eta\eta'\sigma_\delta^2}{\epsilon}}{\kappa}$$

$$\beta_p = \frac{\beta + \frac{\eta^2\sigma_\delta^2}{\epsilon}}{\kappa}, \qquad \gamma_p = \frac{\gamma + \frac{\eta'^2\sigma_\delta^2 + \sigma_{r'}^2}{\epsilon}}{\kappa}$$

$$\kappa \equiv \sqrt{1 + \frac{\sigma_\delta^2}{\epsilon}(\gamma\eta^2 + 2\alpha\eta\eta' + \beta\eta'^2) + \frac{\beta\sigma_{r'}^2}{\epsilon} + \frac{\eta^2\sigma_\delta^2\sigma_{r'}^2}{\epsilon^2}}.$$
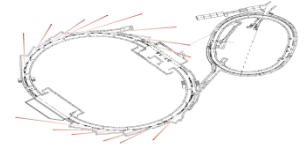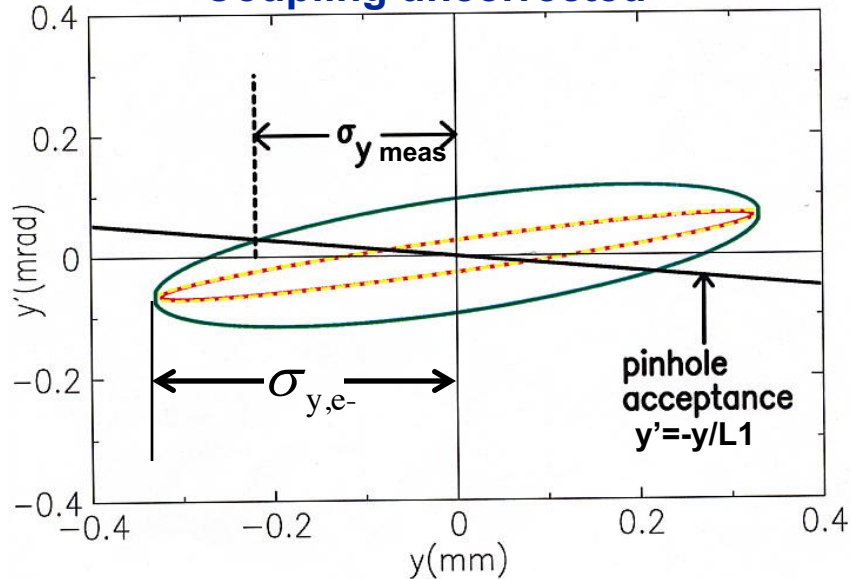

on energy electrons

electrons including energy spread

photons

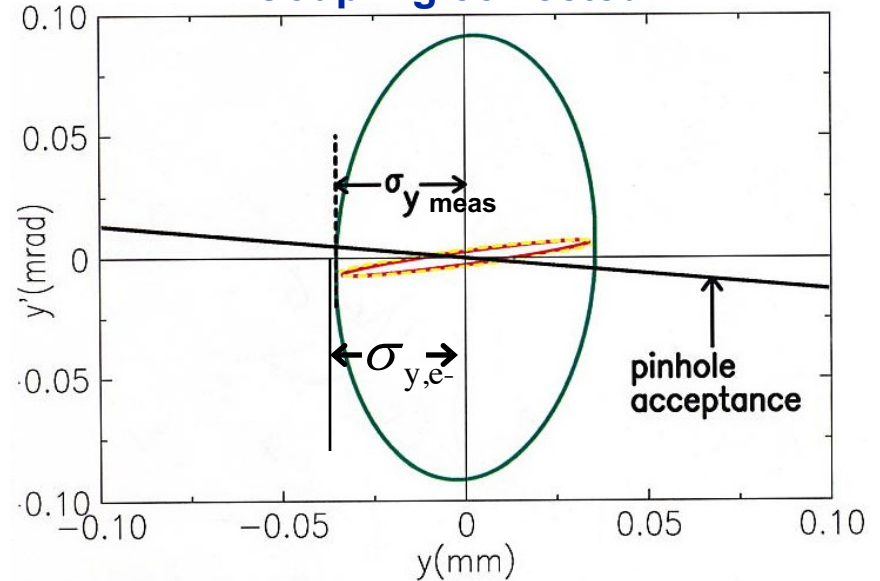$$\sigma_p = \sqrt{\beta\varepsilon + \eta^2\sigma_\delta^2}$$

Measured vertical profile

Coupling uncorrected

Coupling corrected

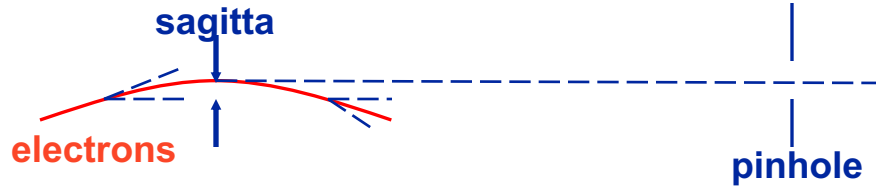The beam profile at the source point seen by the pinhole camera is the intersection of the pinhole camera acceptance, y'=-y/L1, and the photon ellipse. $\sigma_{y,meas} \neq \sigma_{y,e^-}$ The electron emittance can be found with:

$$\varepsilon^2 + B\varepsilon + C = 0$$

$$B = -\sigma^2_{y,meas}(\gamma - 2\alpha/L1 + \beta/L1^2) + \sigma^2_\delta(\gamma\eta^2 + 2\alpha\eta\eta' + \beta\eta'^2) + \beta\sigma^2_{r'}$$

$$C = -\sigma^2_{y,meas}(\sigma^2_{r'} + \sigma^2_\delta(\eta' + \eta/L1)^2) + \eta^2\sigma^2_\delta\sigma^2_{r'}$$

Measured horizontal profile

sagitta

electrons
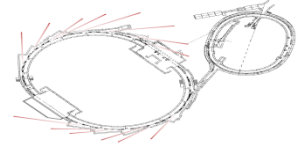
pinhole

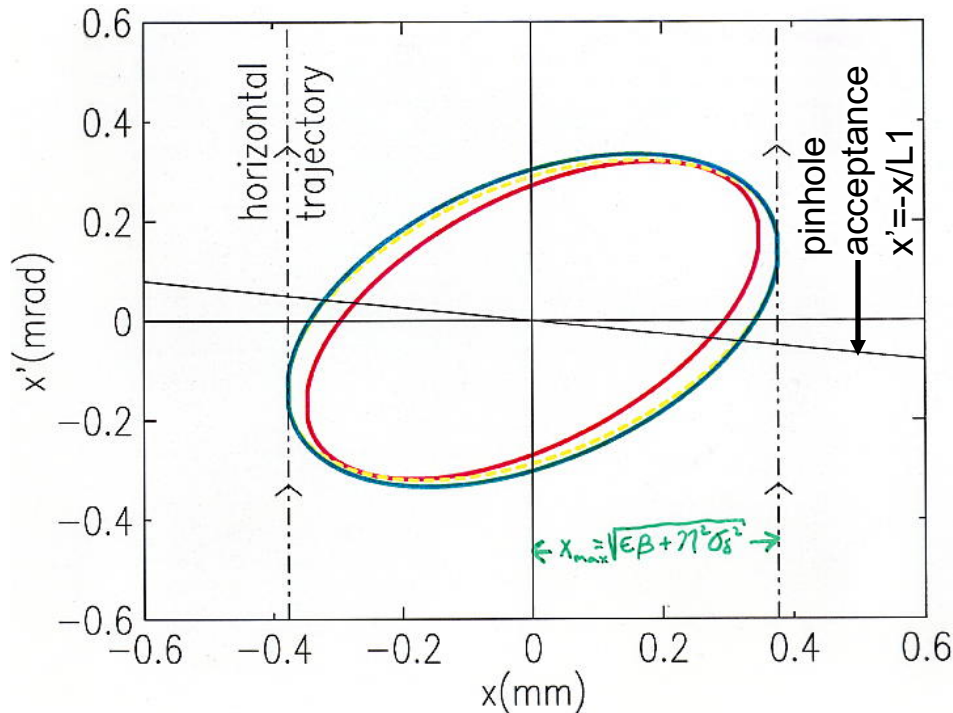**The ellipse sweeps across the pinhole acceptance in an arc in (x,x'). The sagitta (the change in x) is negligibly small.**

horizontal trajectory

pinhole acceptance x'=-x/L1

$x_{max} = \sqrt{\epsilon\beta + \eta^2\sigma_\delta^2}$

x'(mrad)

x(mm)

In the fixed coordinates at the beamline source point, the photon ellipse sweeps across the pinhole acceptance. Integrating the changing profile gives:

$$\int_{-\infty}^{+\infty} dx_0' e^{-(\frac{\gamma_p x^2 + 2\alpha_p x x'(x,x_0') + \beta_p x'^2(x,x_0')}{2\epsilon_p})},$$

$$x'(x, x_0') = x_0' - x/L1.$$
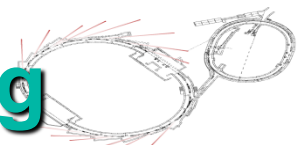
which gives

$$\exp(-\frac{x^2}{2(\epsilon\beta + \eta^2\sigma_\delta^2)}).$$

The integrated profile seen by the pinhole camera is

$$\sigma_{x,meas} = \sqrt{\epsilon\beta + \eta^2\sigma_\delta^2} = \sigma_{x,e-}$$
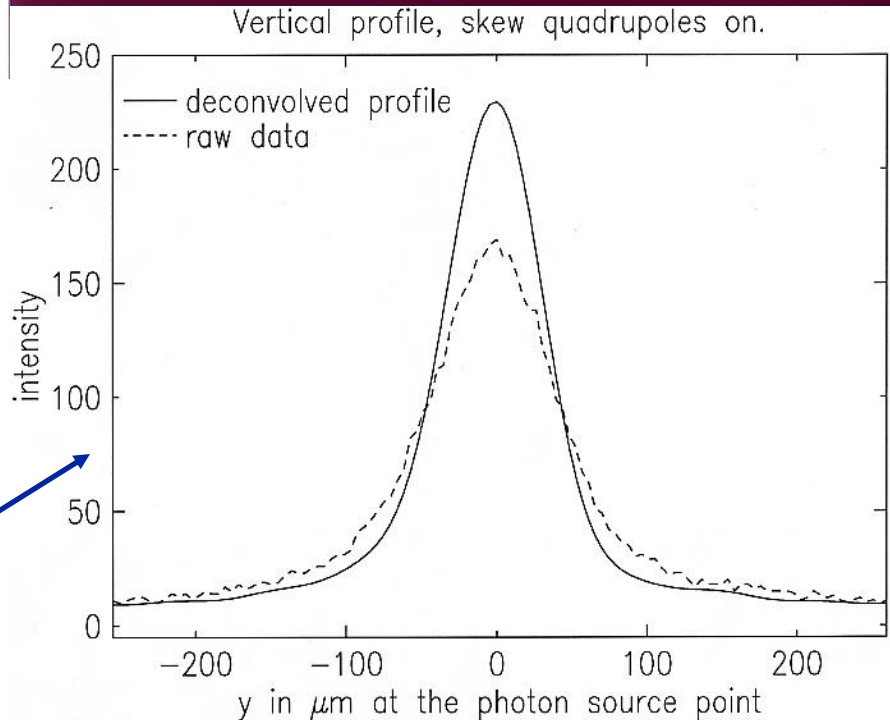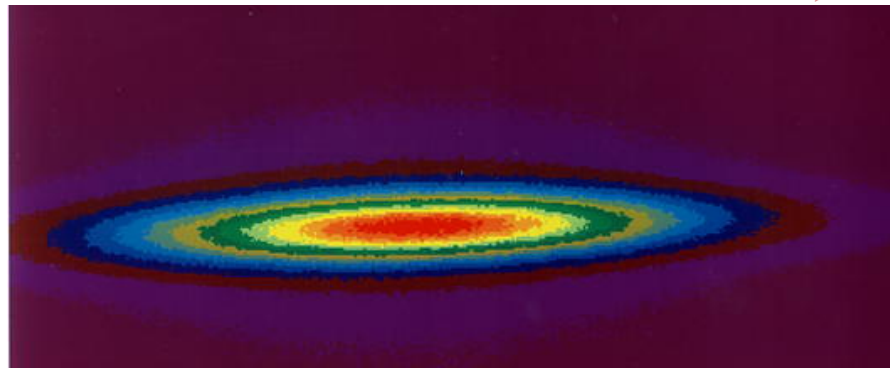
Resolution & image processing

Two contributions to resolution:

1. **Pinhole diffraction.**
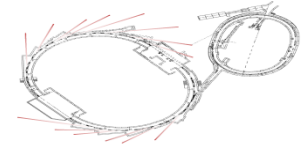
2. **Resolution of detector (phosphor, mirror, lens, and CCD).**

The two resolution functions are deconvolved from each horizontal and vertical slice. A two dimensional, tilted Gaussian is fit to the resulting profile.

Example for one vertical slice.

Vertical profile, skew quadrupoles on.

— deconvolved profile
--- raw data

intensity

y in μm at the photon source point

Diffraction

Even though we are dealing with X-Rays, diffraction is a significant resolution limitation. The diffraction pattern was calculated numerically as a function of pinhole dimension. For large pinholes, it looks like a geometric image of the square pinhole. For small pinholes, it looks like Fraunhofer diffraction, getting larger as the pinhole gets smaller. The pinhole size that gives the best resolution is somewhere between the Fraunhofer regime and geometric image.

Calculating diffraction pattern,

sum up over phases.
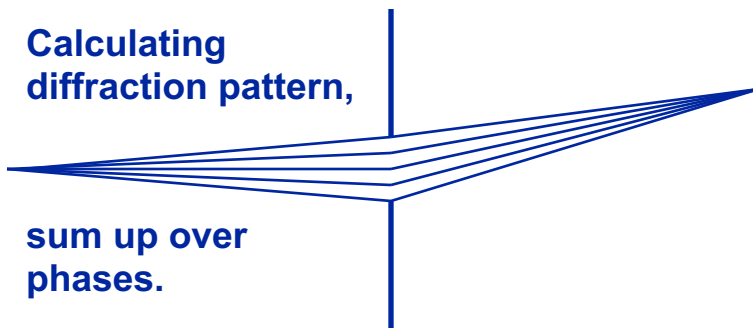
The diffraction pattern must be integrated over the spectrum absorbed by the YAG phosphor.

Power absorbed by .5 mm YAG phosphor after Al foil.
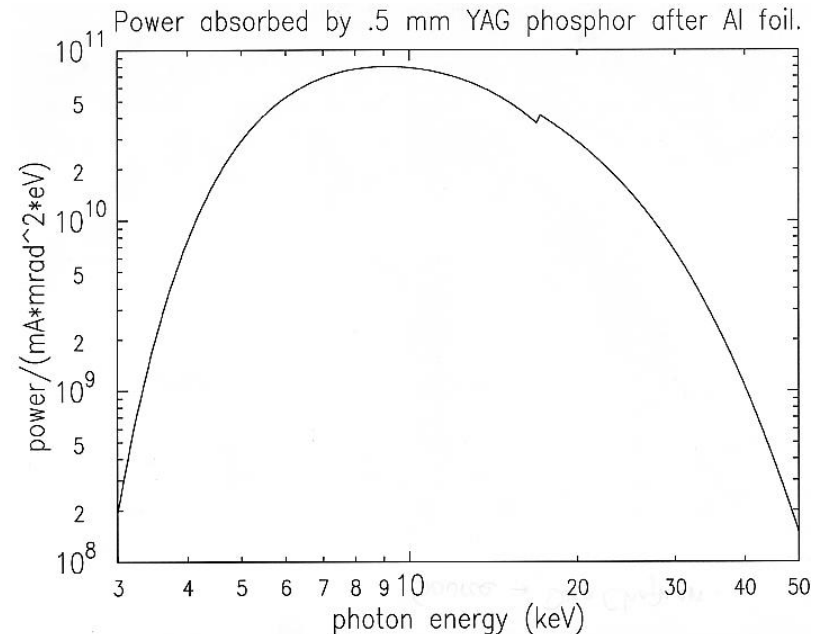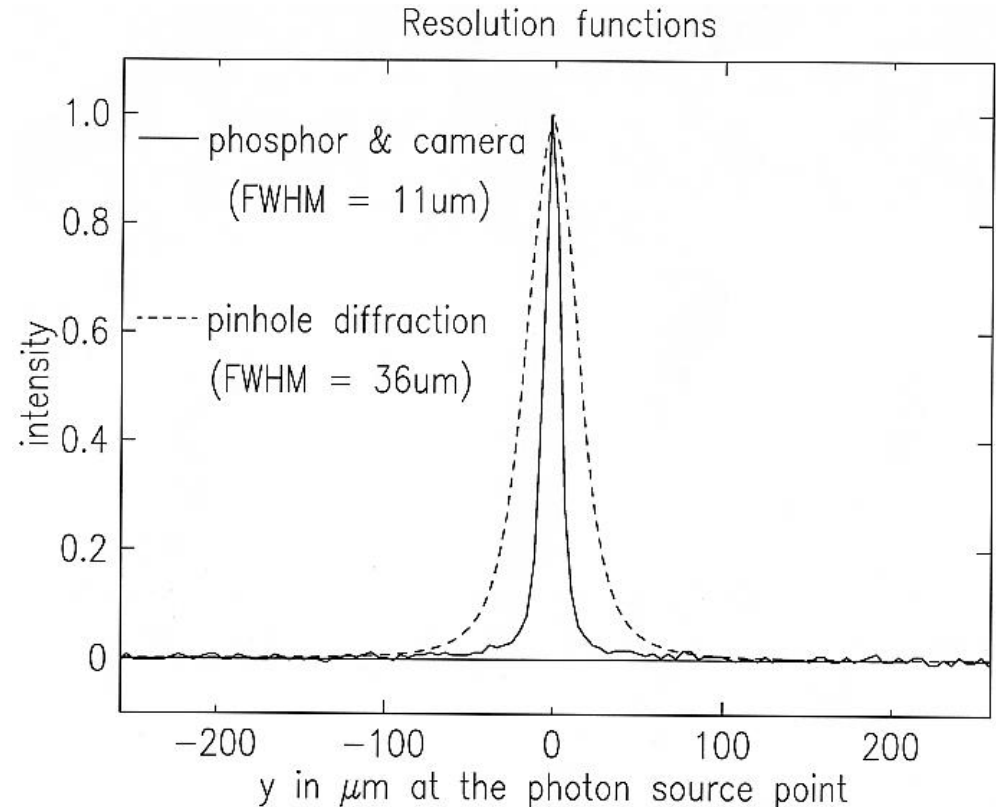
Resolution functions
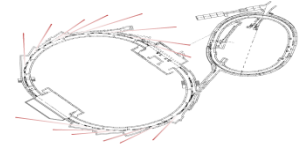
All secondary maxima in the diffraction pattern wash out when integrating over the wavelength spectrum.

The resolution of the detector was measured by placing a very narrow slit just in front of the phosphor.

The measured image is a convolution of the real profile with the resolution functions.

$$I_{\text{meas}} = R \otimes I_{\text{real}}$$

Resolution functions

phosphor & camera (FWHM = 11um)

pinhole diffraction (FWHM = 36um)
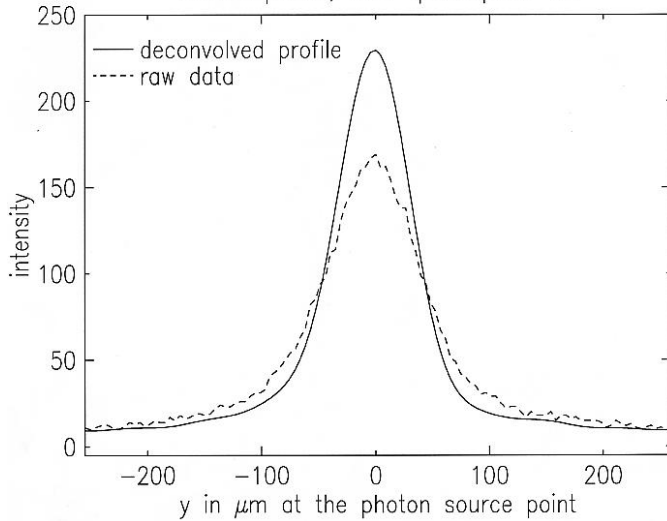
intensity

y in μm at the photon source point

The data and resolution functions are sets of discreet points, so the deconvolution could be turned into a big matrix inversion. A more traditional method uses FFTs. Convolution in frequency space is simply multiplication, so deconvolution becomes division.
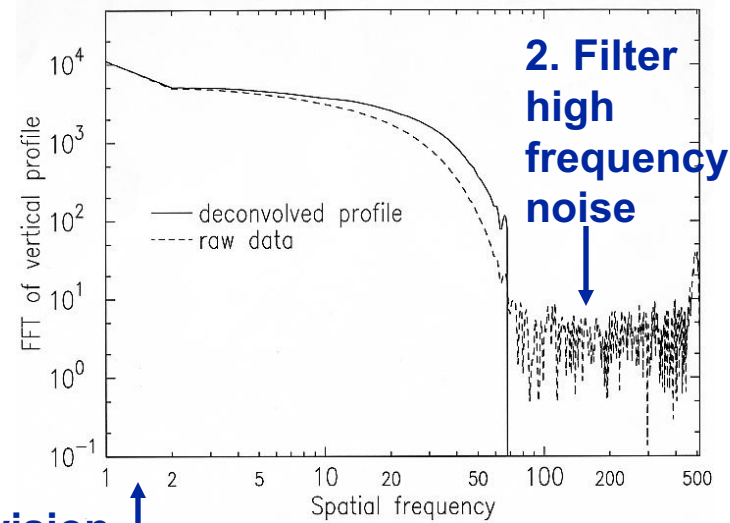
Deconvolution

Vertical profile, skew quadrupoles on.
— deconvolved profile
---- raw data

intensity

y in μm at the photon source point

1. FFT

4. FFT

Spatial frequency amplitude from FFT.

FFT of vertical profile

— deconvolved profile
---- raw data

2. Filter high frequency noise

Spatial frequency

3. division

Resolution functions

intensity

— phosphor & camera (FWHM = 11um)

---- pinhole diffraction (FWHM = 36um)

y in μm at the photon source point
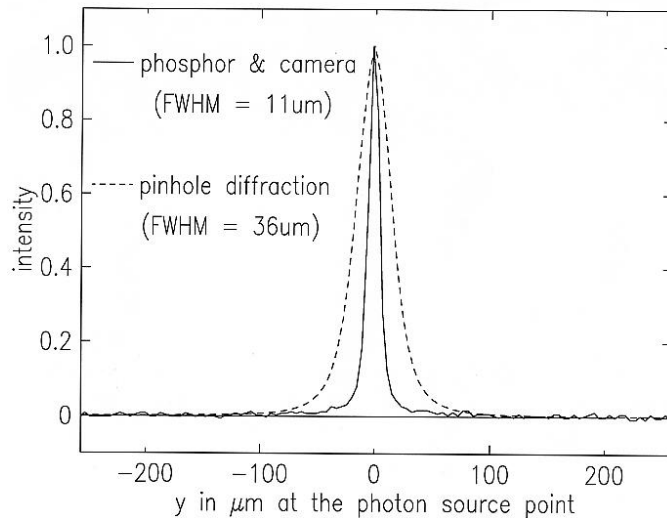
1. FFT

Modulation Transfer Functions

MTF

— phosphor & camera
---- pinhole diffraction

spatial frequency

Beam size measurement   **Beam-based Diagnostics, USPAS, January 21-25, 2019, J. Safranek**
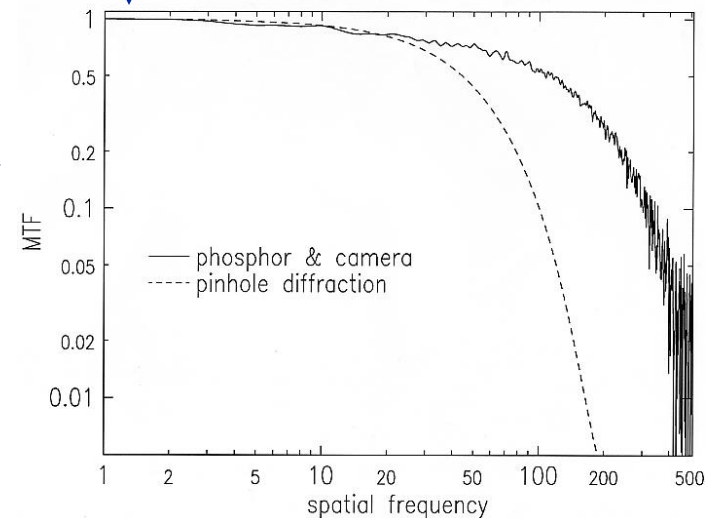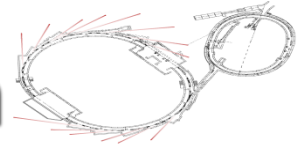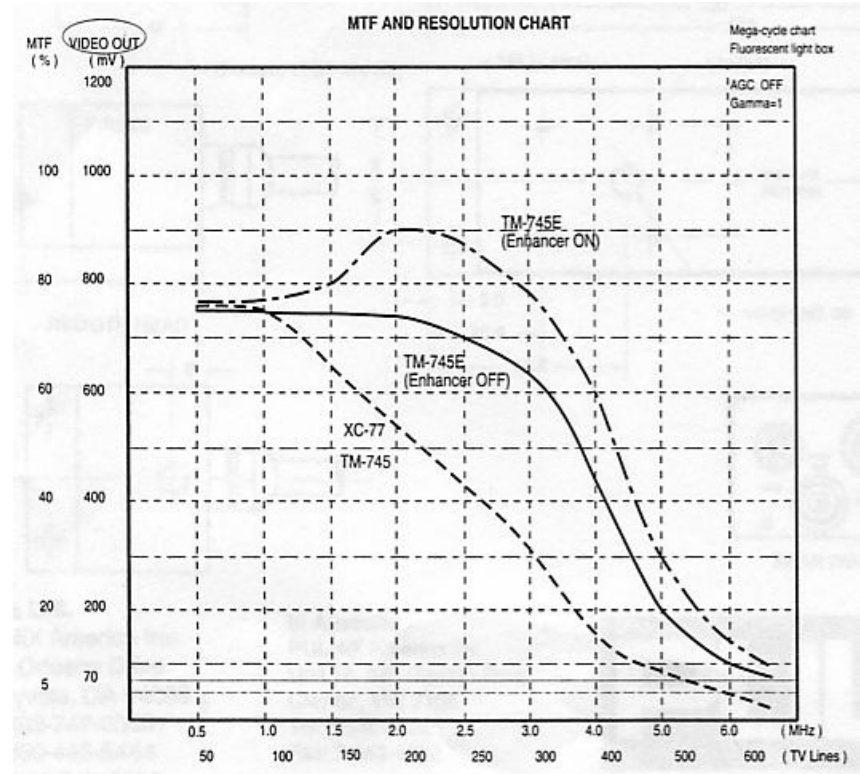
Modulation transfer function

Instead of dividing FFTs, use only amplitude part of FFT – called modulation transfer function (MTF).

MTF is a common way to specify resolution. For example, this graph came with the video camera that was used for the X-Ray Ring pinhole camera.

Pulnix video camera MTF

Numerical Recipes, Cambridge Press, is a good reference for FFTs and deconvolution.